Desalination and Water Treatment
www.deswater.com

doi: 10.5004/dwt.2017.21649

97 (2017) 87–93
November

Evaluation of critical flux and cleaning efficiency for electrospun nanofiber microfiltration membrane

Younghoon Ko, Yongjun Choi, Youngsun Jang, Jihyeok Choi, Sangho Lee*

School of Civil and Environmental Engineering, Kookmin University, Jeongneung-Dong, Seongbuk-Gu, Seoul, 136-702, Korea, Tel. +82 2 910 5060; Fax: +82 2 910 8597; email: sanghlee@kookmin.ac.kr

Received 27 August 2017; Accepted 28 October 2017

ABSTRACT

This study examined fouling characteristics of a commercial grade electrospun nanofiber membrane, which has the nominal pore size of 0.23 μm and the thickness of 165 μm. A set of filtration experiments were carried out in a bench-scale equipment using real wastewater with the mixed liquor suspended solid of 6,500 mg/L. Critical flux was experimentally determined and analyzed using mathematical models such as pore blocking, pore constriction, and cake formation equations. Techniques for physical cleaning of the membrane were applied and compared, including periodic pump stop and backwash. The efficiency of chemical cleaning was measured using NaOCl solutions of different concentrations. Scanning electron microscopy was applied to examine the membrane surfaces before and after chemical cleaning. Results showed that the electrospun membrane has potential for high fouling resistance and effective cleaning. The critical flux seems to exist between 20 and 30 L/m^2 h and the cake formation model resulted in the best fit to the experimental data. The transmembrane pressure increase was reduced by 88% after the application of backwash and the efficiency of chemical cleaning ranged from 84% to 91%.

Keywords: Electrospun nanofiber membrane; Microfiltration; Fouling; Critical flux; Physical cleaning; Chemical cleaning

1. Introduction

Microfiltration (MF) is a particle separation process that has replaced conventional solid–liquid separation process such as sedimentation and media filtration in water treatment. MF is also used as an alternative to secondary clarification in wastewater treatment, allowing the improvement of the existing facility or the new treatment plant [1–4]. Microporous membranes with the pore size ranging from 0.1 to 1 μm are used for MF, which require special techniques for membrane fabrication. For this, it is important to optimize average and maximum pore sizes, pore size distribution, porosity, thickness, and resistances to mechanical and chemical strengths [5]. Phase inversion has been widely adapted for the preparation of MF membranes [5].

Recently, electrospinning has drawn increasing attention as a novel technique for the fabrication of MF membranes [6–8]. Electrospinning technique allows the preparation of microporous membranes consisting of nanofibers [6]. Control of pore size and its distribution as well as the porosity and thickness is attainable by electrospinning technique [7]. This leads to the construction of nanofibrous membranes with high water permeability and narrow pore size distribution [8]. Since scale-up of electrospinning process is still limited, most studies on the electrospun nanofiber MF membranes have been done in bench-scale systems [6–8].

Nevertheless, membrane fouling is one of the most aggravating problems in MF processes for water and wastewater treatment [9–11]. Membrane fouling can be divided into three types according to the characteristics of the foulant: inorganic

* Corresponding author.

fouling, organic fouling, and biofouling [9–11]. Membrane fouling leads to high operating costs by increasing the cleaning frequency and shortening the membrane lifetime [12,13]. It is necessary to accurately predict membrane fouling by applying either hydrodynamic or statistical models for preventive maintenance [14–16].

Although many works have been carried out to address fouling problems in conventional MF membranes prepared by phase inversion, relatively little information is available on fouling of electrospun nanofiber MF membranes [6,7], which may have different fouling propensity due to their different structures. Accordingly, this study focused on the evaluation of fouling characteristics and cleaning efficiency for flat sheet electrospun membranes. Real wastewater was used as the feed solution. Critical flux was measured and the results were analyzed by applying filtration model equations. Conditions for physical/chemical cleaning methods were compared. The originality of this study lies in its attempts to elucidate fouling mechanisms and determine proper methods for physical and chemical cleaning for commercial grade MF membranes fabricated by electrospinning technique.

2. Material and methods

2.1. Feed water

The feed water used in this study was the wastewater from an aerobic reactor of a membrane bio-reactor system in the Guri City sewage treatment plant in Korea. The water quality parameters are summarized in Table 1. The wastewater was taken once a week and replaced every 3–4 d.

2.2. Membrane

The electrospun MF membranes were supplied by a membrane manufacturer (AMOGREENTECH, Korea). Membrane material is polyvinylidene fluoride as a mesh laminate type. The pore size and the thickness were 0.23 μm and 165 μm, respectively. A plate-and-frame module was chosen to use the membranes in a submerged filtration configuration. The module had two flat sheet MF membranes attached on both sides of a supporting panel with a tube to a permeate water line. The effective membrane area of the module was 0.0689 m^2.

2.3. Experimental setup and conditions

Fig. 1 shows the schematic diagram for a bench-scale MF system. The plate-and-frame MF module was submerged into the feed tank. Aeration was carried out using an aerator (air stone) at the bottom of the tank. An air pump was used with the air flow meter to supply a given amount of air. A permeate pump was used to provide the pressure required to obtain the imposed flux through the membrane. The transmembrane pressure was continuously measured using an electronic pressure sensor connected to a computer. To ensure the constant flux operation, the mass of the permeate was measured using an electronic balance. Total recycle operation was used and thus the permeate was periodically returned to the feed tank. The volume of the feed tank was 20 L, the stirrer was set at 300 rpm, and the air flow rate was set at 0.1 mL/min.

Table 1
Water quality parameters

Category	Wastewater
pH	7.8
DO, mg/L	1.5
TOC, mg/L	19.55
SS, mg/L	6,500
Turbidity, NTU	141
Conductivity, mg/L	751

Experiments were carried out through the following steps. First, the membrane resistance was measured using distilled water at a flow rate of 10–50 LMH (L/m^2 h) for 2 h each step. All membrane modules were measured before filtration and backwash experiments to ensure the reliability of the experiment. Then, the critical flux was measured using the feed water by applying the flux step method. After the membrane fouling occurred, physical cleaning methods including periodic pump stop and backwash were applied and compared. In this case, the backwash was performed at 1.5 times the flow rate of the filtration. Finally, the chemical cleaning was carried out using NaOCl solutions of different concentrations when the transmembrane pressure reached a certain pressure (0.3, 0.6, 0.9 bar). Sodium chlorate (NaOCl) was used as a chemical cleaning agent, and the concentrations were 250, 500, and 1,000 mg/L, respectively. Prior to chemical cleaning, the membrane module was immersed in a bath containing deionized (DI) water and then backwashed using DI water. Then the following steps were applied: (1) the module was submerged for 10 min in chemical agent tank, (2) it was backwashed for 10 min in chemical agent tank, (3) the remaining solution in the tank was replaced with DI water, and (4) the module was backwashed again for 10 min with DI water.

2.4. Analytical methods

The pH and conductivity were measured using a Multi 3420 (Wissenschaftlich-Technische Werkstätten GmbH, Germany) digital precision meter. Turbidity was measured using a portable Turb 430 IR (Wissenschaftlich-Technische Werkstätten GmbH, Germany) turbidimeter. The dissolved oxygen (DO) was measured by portable DO meter (Hach Lange HQ40d Multimeter). The total organic carbon (TOC) was measured using a TOC analyzer (DC-180,

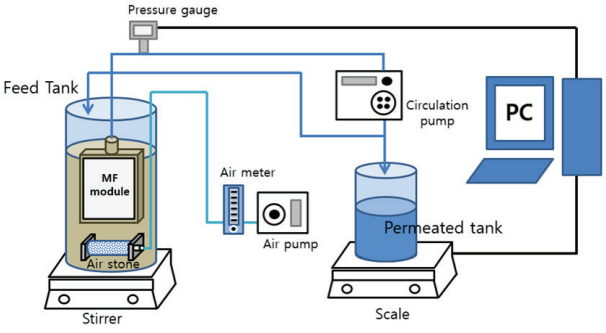

Fig. 1. Laboratory-scale MF device.

Rosemount, USA). Each water quality analysis was measured immediately after the end of the experiment. Membrane structures and surfaces were closely analyzed using field emission electron microscopy (JSM-7610F, JEOL Ltd., Japan).

3. Modeling approach

The model for membrane fouling can be divided into static pressure transmission model and constant flow transmission model. In the static pressure transmission model, the transmembrane pressure (TMP) maintains constant and the permeation flux decreases as the membrane fouling progress. On the contrary to this, in the constant flow transmission model, the permeation flux maintains constant and the TMP changes as the membrane fouling progress. Therefore, in the static pressure transmission model, TMP is an independent variable and the permeation flux is a dependent variable, which can be expressed by the same model as Eq. (1). On the other hand, in the constant flow permeation model, it can be expressed by a model like Eq. (2). In Eqs. (2) and (3), applicable models can be classified according to the value of n. For example, there are complete pore blocking (n = 2), standard pore blocking (n = 1.5), intermediate pore blocking (n = 1), and cake formation (n = 0) [17].

$$\frac{\mathrm{d}^2t}{\mathrm{d}V^2} = k\left(\frac{\mathrm{d}t}{\mathrm{d}V}\right)^n \tag{1}$$

$$\frac{\mathrm{d}^2t}{\mathrm{d}(\Delta P)^2} = k\left(\frac{\mathrm{d}t}{\mathrm{d}(\Delta P)}\right)^n \tag{2}$$

$$Q_l = \frac{\Delta P A_{\mathrm{mem}}}{\mu R_m} \tag{3}$$

where t is time (min), V is volume (m^2), k and n are the parameters of fouling model, ΔP is the pressure (kPa), Q_l is the volume flow rate, R_m is membrane resistance (1/m), and μ is the viscosity (Pa s). The permeation flux equation (Eq. (3)) derived from the Darcy's law was substituted for the membrane fouling model (Eq. (2)) for constant flow permeation and it can derive three types of membrane fouling model as shown in Table 2 by integrating each permeation model assumed below [16].

P_o is the initial transmembrane pressure; J is the operating flux; J_c is the critical flux; C_b is the concentration of deposits in bulk phase; and α, β, and γ are model constants, respectively.

Table 2
Membrane fouling model

Models	Integral forms	
Pore blocking model	$\Delta P(t) = P_o\left(1 - \frac{\alpha(J - J_c)C_b t}{A_{\mathrm{mem}}}\right)^{-1}$	(4)
Pore constriction model	$\Delta P(t) = P_o\left(1 - \beta(J - J_c)C_b t\right)^{-2}$	(5)
Cake formation model	$\Delta P(t) = P_o + \gamma(J - J_c)^2 \mu C_b t$	(6)

The following two conditions are assumed for model derivation. First, the particle deposition occurs only when $J(t)$ exceeds J_c. Second, only one fouling model predominates in each case. Prediction of the fouling model was based on root mean square error, the most widely used criterion.

4. Results and discussions

4.1. Membrane characterization

As mentioned previously, the commercial grade electrospun nanofiber membranes were used in this study. The average R_m value of the membrane module was determined to be 2.9 × 10^{11} m^{-1}. This corresponds to the water pemeability ($J/\Delta P$) of 1,517 L/m^2 h bar at 20°C. This value is similar to the water permeabilities of MF membranes rainging from 500 to 2,000 L/m^2 h bar, which are fabricated by phase inversion methods [5]. Scanning electron microscopy (SEM) image analysis was also carried out as shown in Fig. 2. Results showed that the electrospun membrane consisted of nanofibers that have the diameter ranging from 50 to 200 nm. The surface morphology appears to be quite different from those of the MF membranes from the phase inversion methods [5].

4.2. Permeate water quality

Water quality analysis of permeate water was carried out after MF operation in real wastewater condition. The turbidity of wastewater was 141 NTU due to high mixed liquor suspended solid. The turbidity of permeate water was 0.40 NTU (99.7% removed) and most of the suspended matter was removed. The TOC of the permeate water was 0.77 mg/L (96.1% removed), indicating a high removal rate. Due to the nature of the MF process, dissolved ions were passed through the membrane and the conductivity was measured at 740 mg/L similar to that of the raw water.

4.3. Critical flux and model fits

The flux-step method was applied to determine the critical flux of the membrane module for the real wastewater. The experiments were carried out by changing the flux

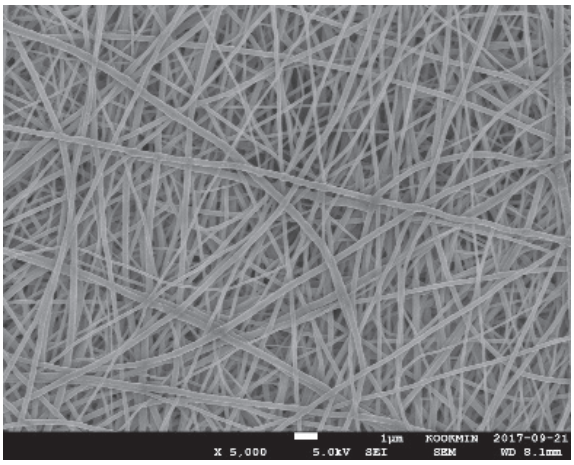

Fig. 2. Scanning electron microscopy (SEM) of electrospun membrane.

(suction flow rate) from 10 to 30 L/m² h. The stirring speed was adjusted from 100 to 400 rpm but resulted in negligible effect so the results were not included here. Fig. 3 shows the variations of the flux with time at different flux values. The operating time is 24 h. In case of flux, 10 and 20 LMH (L/m² h) in Figs. 3(a) and (b), the TMP did not significantly increase. In Fig. 3(c), the TMP rapidly increased from the beginning and reached up to about 0.4 bar. Therefore, it appears that the critical flux exists between 20 and 30 L/m² h.

The pore blocking model, the pore constriction model, and the cake formation model were applied for the determination of accurate critical flux values and the dominant fouling mechanism. The model equations are summarized in Table 2. Fig. 4 compares the results of three model fits with the experimental data. The model parameters and R^2 values are shown in Table 3. It is evident from the results that the cake formation model matched the experimental results well. On the other hand, the other models only provided poor fittings. Based on the fitting to the cake formation equation, the critical flux was determined to be 24 L/m² h.

4.4. Physical cleaning

Physical cleaning methods including periodic stop of filtration pump and backwash were applied and the increasing rates of TMP were compared. The results are illusrated in Fig. 5. The filtration without any physical cleaning resulted in

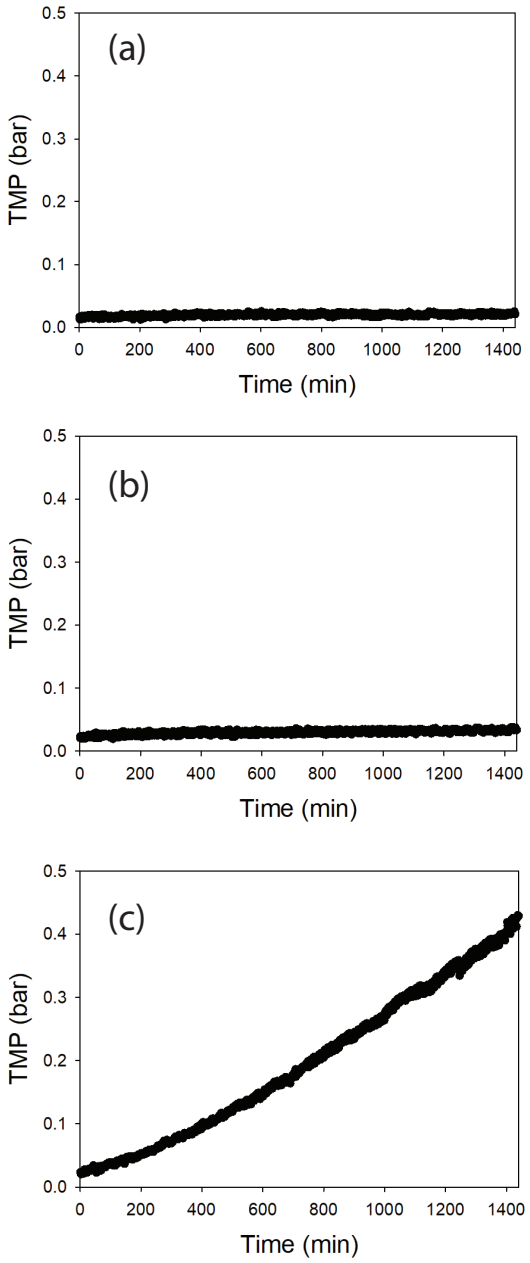

Fig. 3. Graphs of experiment result at (a) 10, (b) 20, and (3) 30 L/m² h of flux.

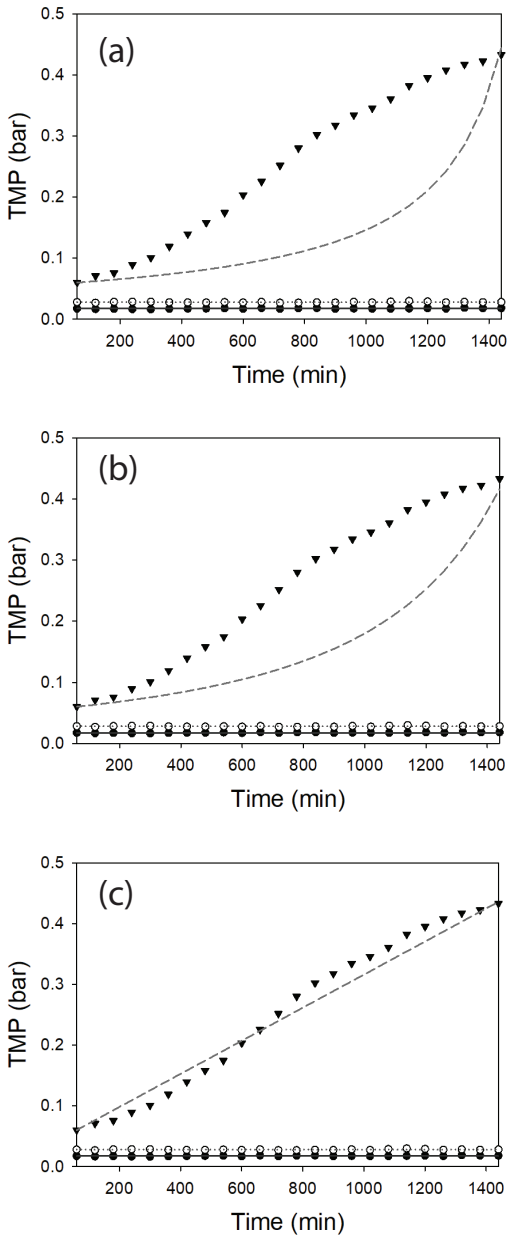

Fig. 4. Graphs of critical flux models: (a) pore blocking model, (b) pore constriction model, and (c) cake formation model.

Table 3
Model parameters and R^2 values

Fouling models	Model constants (α, β, and γ)	Critical flux (J_c)	$R^2 = \sum (TMP_{exp} - TMP_{model})^2$
Pore blocking model	3.7 m^4/kg	24	1.19×10^{-4}
Pore constriction model	33 m^2/kg	23	2.91×10^{-4}
Cake formation model	1.40×10^{10} m/kg	24	8.80×10^{-6}

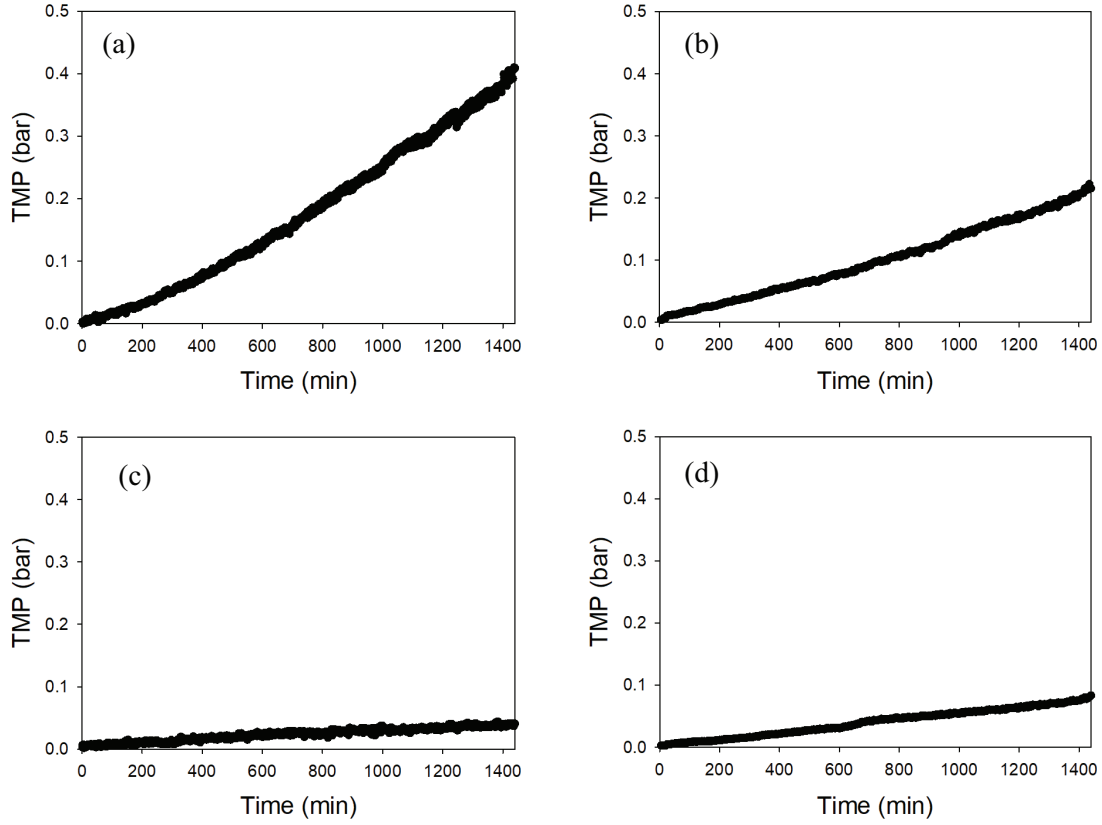

Fig. 5. Graphs of physical cleaning: (a) continuous filtration, (b) filtration and pump stop (7 min/20 s), (c) filtration and backwashing I (7 min/20 s), and (d) II (14 min/20 s).

the highest rate of TMP increase, which was 0.37 ± 0.05 bar/d. The application of periodic pump stop could reduce the rate of TMP increase by 43% (0.21 ± 0.05 bar/d). The backwash was more effective to decrease the TMP. With the filtration interval of 7 min and backwash duration of 20 s, the rate of TMP increase was reduced by 79% (0.045 ± 0.005 bar/d). An increase in the filtration interval twice (14 min) resulted in the rate of TMP increase of 0.095 ± 0.015 bar/d, which is still significantly lower than the filtration without the physical cleaning. Since frequent backwash can result in a large loss in product water, the backwash interval should be optimized by simultaneously considering the physical cleaning efficiency and product water recovery [18,19].

It should be noted that backwash is generally accepted by hollow fiber MF membranes rather than flat sheet MF membranes [5]. This is because most flat sheet MF membranes prepared by phase inversion may not have enough mechanical strength to allow the application of backwash1. However, it is possible to implement backwash in flat sheet MF membranes fabricated through electrospinning due to their high mechanical strengths. This is one of the advantages with the use of electrospun membranes to allow anti-fouling capability.

4.5. Chemical cleaning

Although physical cleaning is effective, the permeability of MF membranes should be eventually recovered by applying chemical cleaning. Accordingly, the efficiency of chemical cleaning using NaOCl was examined. As mentioned previously, the effect of NaOCl concentration and final TMP on the recovery of membrane permeability was investigated. The results are summarized in Fig. 6. When the final TMP was 0.3 bar (Fig. 6(a)), the TMP recovery ratio was higher than 91%, indicating that the chemical cleaning is effective to control fouling. With the increase in the final TMP to 0.6 and 0.9 bar (Figs. 6(b) and (c)), the minimum recovery ratio was reduced to 84%. The NaOCl concentration also affected the

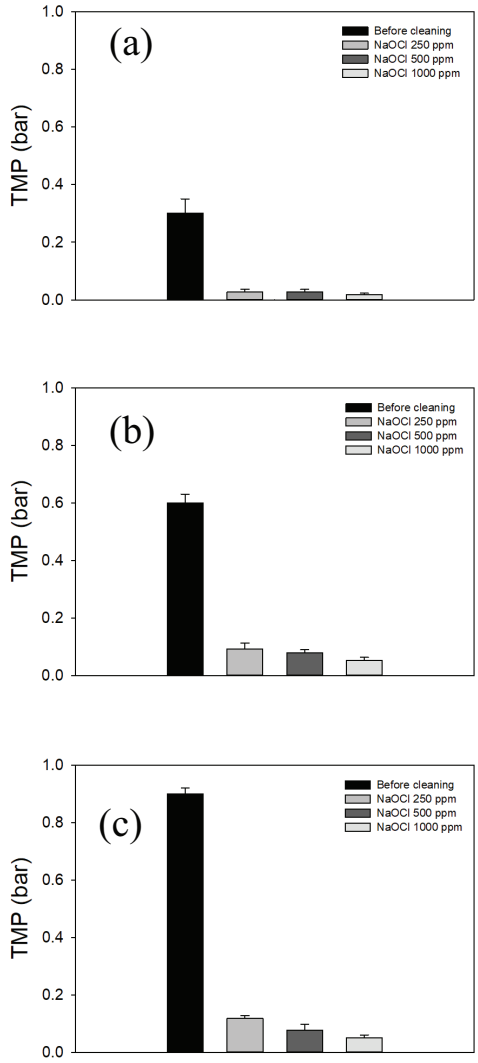

Fig. 6. Graphs of chemical cleaning in TMP (a) 0.3, (b) 0.6, and (c) 0.9 bar.

TMP recovery ratio but the effect was more important with higher final TMP value. The effect of NaOCl concentration on the TMP recovery ratio was negligible at the final TMP of 0.3 bar but it became significant at the final TMP of 0.9 bar. In other words, higher concentration of cleaning solution is required when the fouling is more serious.

The SEM images of the membrane surface were compared before and after chemical cleaning with the NaOCl concentration of 250 mg/L and final TMP of 0.6 bar. As shown in Fig. 7(a), the membrane surface was covered by thick cake layer after the filtration experiment and before the chemical cleaning. As indicated by the model fit in Table 3, the SEM image confirms that the cake formation is the major fouling mechanism. After the chemical cleaning, the surface of the membrane became clean as demonstrated in Fig. 7(b). The cake layer was removed and the surface pores were exposed. No foulants were visually found inside the membrane pores from the SEM image. This suggests that the electrospun MF membrane is relatively easy to be cleaned using NaOCl solution in the case of wastewater treament.

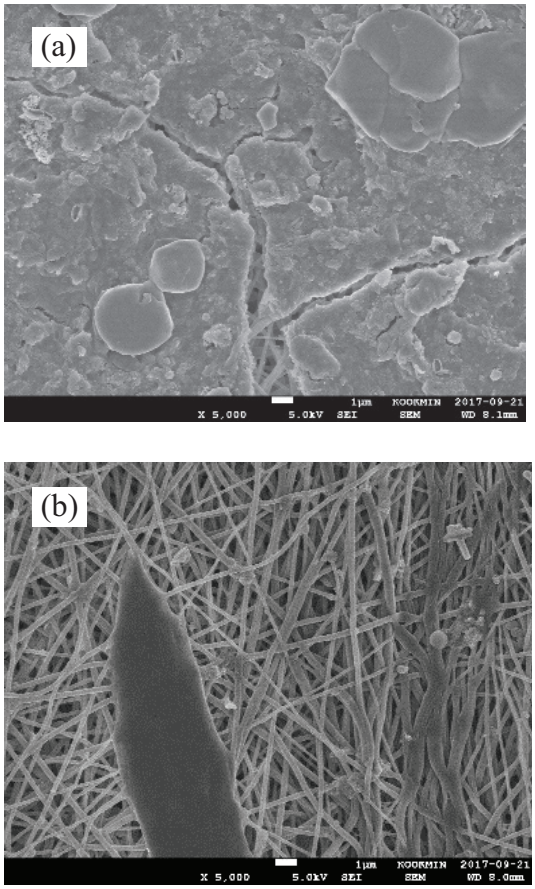

Fig. 7. SEM images for (a) membrane before cleaning and (c) membrane after cleaning.

5. Conclusions

In this study, fouling characteristics and cleaning efficiency of flat sheet electrospun nanofiber MF membranes were investigated for wastewater treatment. The following conclusions were drawn:

- The electrospun membrane had the intrinsic membrane resistance of 2.9×10^{11} m^{-1}, which corresponds to the water pemeability ($J/\Delta P$) of 1,517 L/m^2 h bar at 20°C. The SEM image analysis indicated that the electrospun membrane consisted of nanofibers with the diameter between 50 and 200 nm.
- The critical flux for the wastewater treatment was determined to be around 20–30 L/m^2 h. The model fit suggested that cake formation is the dominant fouling mechanism with the calculated critical flux of 24 L/m^2 h.
- The backwash was effective to suppress the increase in TMP during the filtration. The increasing rates of TMP were 88% with the backwash interval of 7 min and 74% with the backwash interval of 14 min, respectively.
- The chemical cleaning using NaOCl with the concentration between 250 and 1,000 mg/L was found to be effective to recover the water permeability of the membrane. With the final TMP of 0.3 bar, the TMP recovery ratio was higher than 91% and with the final TMP of 0.6 and 0.9 bar, the TMP recovery ratio was over 84%.

Acknowledgment

This subject is supported by Korea Ministry of Environment as "Global Top Project (2017002100001)."

References

[1] I.H. Cho, J.T. Kim, Trends in the technology and market of membrane bioreactors (MBR) for wastewater treatment and reuse and development directions, Membr. J., 23 (2013) 22–24.
[2] J.T. Kim, H. Hwang, B. Hong, H. Byun, The background and direction of R&D project for advanced technology of wastewater treatment and reuse, Membr. J., 21 (2011) 277–289.
[3] H. Monclús, J. Sipma, G. Ferrero, J. Comas, I. Rodriguez-Roda, Optimization of biological nutrient removal in a pilot plant UCT-MBR treating municipal wastewater during start-up, Desalination, 250 (2010) 592–597.
[4] H. Monclús, J. Sipma, G. Ferrero, I. Rodriguez-Roda, J. Comas, Biological nutrient removal in an MBR treating municipal wastewater with special focus on biological phosphorus removal, Bioresour. Technol., 101 (2010) 3984–3991.
[5] B.S. Lalia, V. Kochkodan, R. Hashaikeh, N. Hilal, A review on membrane fabrication: structure, properties and performance relationship, Desalination, 326 (2013) 77–95.
[6] X. Wang, B.S. Hsiao, Electrospun nanofiber membranes, Current Opin. Chem. Eng., 12 (2016) 62–81.
[7] Y. Ding, H. Hou, Y. Zhao, Z. Zhu, H. Fong, Electrospun polyimide nanofibers and their applications, Progr. Polym. Sci., 61 (2016) 67–103.
[8] F.E. Ahmed, B.S. Lalia, Raed Hashaikeh, A review on electrospinning for membrane fabrication: challenges and applications, Desalination, 356 (2015) 15–30.
[9] P. Le-Clech, V. Chen, T.A.G. Fane, Fouling in membrane bioreactors used in wastewater treatment, J. Membr. Sci., 284 (2006) 17–53.
[10] H.C. Flemming, Biofouling in water systems – cases, causes and countermeasures, Appl. Microbiol. Biotechnol., 59 (2002) 629–640.
[11] I. Rosas, S. Collado, A. Gutiérrez, M. Díaz, Fouling mechanisms of *Pseudomonas putida* on PES microfiltration membranes, J. Membr. Sci., 465 (2014) 27–33.
[12] G. Ferrero, H. Monclús, G. Buttiglieri, J. Comas, I. Rodriguez-Roda, Automatic control system for energy optimization in membrane bioreactors, Desalination, 268 (2011) 276–280.
[13] S. Judd, The MBR Book, Principles and Applications of Membrane Bioreactors for Water and Wastewater Treatment, Elsevier, Oxford, UK, 2011.
[14] H. Monclús, G. Ferrero, G. Buttiglieri, J. Comas, I. Rodriguez-Roda, Online monitoring of membrane fouling in submerged MBRs, Desalination, 277 (2011) 414–419.
[15] H. Kaneko, K. Funatsu, Physical and statistical model for predicting a transmembrane pressure jump for a membrane bioreactor, Chemom. Intell. Lab. Syst., 121 (2013) 66–74.
[16] Y. Choi, H. Oh, S. Lee, Y. Choi, T. Hwang, G. Baek, Y. Choung, Large-pore membrane filtration with coagulation as an MF/UF pretreatment process, Desalination, 15 (2010) 149–159.
[17] C.Y. Ng, A.W. Mohammad, L.Y. Ng, J.M. Jahim, Membrane fouling mechanisms during ultrafiltration of skimmed coconut milk, J. Food Eng., 142 (2014) 190–200.
[18] E. Zondervan, B.H.L. Betlem, B. Blankert, B. Roffel, Modeling and optimization of a sequence of chemical cleaning cycles in dead-end ultrafiltration, J. Membr. Sci., 308 (2008) 207–217.
[19] G. Mannina, A. Cosenza, The fouling phenomenon in membrane bioreactors: assessment of different strategies for energy saving, J. Membr. Sci., 444 (2013) 332–344.